Recent Development and Application of Magnetic Nanoparticles for Cell Labeling and Imaging

Chao Zhang[1,2], Tao Liu[1], Jining Gao[1], Yongping Su[1] and Chunmeng Shi*[,1]

[1]*Institute of Combined Injury, State Key Laboratory of Trauma, Burns and Combined Injury, Chongqing Engineering Research Center for Nanomedicine, College of Preventive Medicine, Third Military Medical University, Chongqing, China*

[2]*Department of Orthopedics, Xinqiao Hospital, Third Military Medical University, Chongqing, China*

Abstract: Magnetic iron oxide nanoparticles have attracted extensive interest as novel contrast agents for biomedical imaging owing to their capability of deep-tissue imaging, non-invasiveness and low toxicity. This mini-review will provide an overview on the recent synthesis methods, influencing factors and potential applications of magentic nanoparticles for cell labeling and imaging.

Keywords: Superparamagnetic iron oxide nanoparticles, magnetic nanoparticles, cell tracking, cytotoxicity, targeted imaging.

INTRODUCTION

Magnetic resonance imaging (MRI) is the most used non-invasive imaging modality for *in vivo* cell tracking and imaging in biomedical applications because of its safety and 3-dimensional capabilities. This technique is based on nuclear magnetic resonance (NMR), a spectroscopic technique which is used for obtaining microscopic chemical and physical information about molecules. Exogenous contrast agents are often used to enhance the sensitivity and specificity of MRI. Superparamagnetic iron oxide nanoparticles (SPIOs) have a long blood-retention time and are more sensitive than most frequently used contrast agent gadolinium (Gd^{3+}). SPIOs are becoming increasingly attractive for the development of novel MRI contrast agents. In the past few years, several forms of SPIOs have been applied in clinical settings and have proven to be safe in human use [1, 2]. This mini-review article will summarize the current advances on the development and application of SPIOs for cell labeling and imaging. The physicochemical properties, synthetic strategies, applications and safety related issues will be discussed.

SUPERPARAMAGNETIC IRON OIXDE NANOPARTICLES

Superparamagnetism is a unique physical phenomenon which takes place in small ferromagnetic or ferrimagnetic nanoparticles and have magnetic dipole characteristics of both paramagnetism and ferrimagnetism [3]. It can be understood by considering the behavior of a well-isolated single-domain particle which can randomly flip direction under external magnetic field. When the external magnetic field disappears, the ferrimagnetic dipole orientation more closely resembles a paramagnetic material with a random dipole orientation and zero magnetization. However, their magnetic susceptibility is much larger than the one of paramagnets [4-6]. SPIO nanoparticle is a conglomerate of numerous iron oxide crystals coated with coating materials. Coatings can maintain the stability of SPIOs in colloidal suspension and make these nanoparticles soluble in water [7]. Under an external magnetic field, SPIOs can create very high local magnetic field gradients by inducing water proton spin dephasing and loss of T2-weighted enhancement signal intensity in the accumulated region was observed [3, 7]. Following the increase of particle size, the superparamagnetism of SPIOs will be changed into ferrimagnetism.

The hydrodynamic size of SPIOs can vary widely depending on the type of synthesis and surface modification. The particle size plays a critical role in determining the magnetic and biological properties. Currently, a variety of SPIOs have been developed and used depending on the hydrodynamic size, such as larger oral SPIO agents (approximately 300 nm-3.5 μm), standard SPIO (SSPIO, approximately 60-150 nm), ultra-small SPIO (USPIO, approximately 10-50 nm), and very small SPIO (VSOP, approximately ~10nm) [8, 9]. In addition, there is a subset of USPIO with a single crystal core named monocrystalline iron oxide nanoparticles (MION, approximately 10-30 nm) which only has a single iron oxide crystal core [10]. In order to avoid confusion, the term SPIOs will be used to cover all SSPIO ,USPIO, MION, and VSOP in this article. Table **1** summarizes several commercial available and pre-clinical SPIO nanoparticles.

SYNTHESIS OF IRON OXIDE NANOPARTICLES

In the last decades, much effort has been devoted to the synthesis of magnetic nanoparticles with a number of different compositions and phases. The surface properties of iron oxide particles play an important role in governing the fate of the nanoparticles *in vivo* apart from providing the underlying particles with the necessary water-solubility and colloidal stability under physiological conditions. This is usually

*Address correspondence to this author at the Institute of Combined Injury, State Key Laboratory of Trauma, Burns and Combined Injury, Third Military Medical University 30 Gaotanyan Road, Chongqing, 400038, China; Tel: 86-23-68752280; E-mail: shicm1010@yahoo.com.cn

1389-5575/10 $55.00+.00

Table 1. Characteristics of Commercial Available and Pre-Clinical Utilized SPIOs

Names	Company	Applications	Coatings	Core size	Total size	Relaxometric properties $mM^{-1} s^{-1}$	Refs.
AMI-25 (Feridex; Endorem, ferumoxides)	Guerbet; Advanced Magnetics	Cellular labeling; Liver imaging	Dextran T10	5-6nm	80-150nm	r_1=10.1; r_2=120, B_0=1.5T	[70]
AMI-227 (Combidex; Sinerem)	Guerbet; Advanced Magnetics	Lymph node imaging; Macrophage imaging and Cellular labeling	Dextran	4-6nm	20-40nm	r_1=9.9; r_2=65, B_0=1.5T	[71]
SHU-555A (Resovist;Ferucarbotran)	Schering	Cellular labeling	Carboxydextran	4nm	60nm	r_1=9.7; r_2=189, B_0=1.5T	[72]
SHU-555C(Supravist®)	Schering	Cellular labeling; Blood pool agent	Carboxydextran	~5	20nm	r_1=10.7; r_2=38, B_0=1.5T	[73]
Ferumoxytol Code 7228	Advanced Magnetics	Macrophage imaging; Blood pool agent; Cellular labeling	Carboxylmethyl-dextran	~7nm	30nm	r_1=15; r_2=89, B_0=1.5T	[74]
AMI-121(Ferumoxsil Lumirem®/Gastromark®)	Guerbet; Advanced Magnetics	Bowel MR imaging	Siloxane	10nm	300nm	r_1=3.4, r_2=3.8, B_0=1.0T	[75]
VSOP-C184	Ferropharm	Blood pool agent; Cellular labeling	Citrate	4nm	7nm	r_1=20.1, r_2=37.1, B_0=0.94 T	[76]
Feruglose NC100150 PEG-feron Clariscan™	GE-Healthcare	Blood pool agent, Vascular imaging	PEG	4-7nm	20nm	r_1=20, r_2=35, B_0=0.5T	[77]
MION	Preclinical	MR angiography; Targeted imaging; Cellular labeling	Dextran	4.6nm	20nm	r_1=16.5, r_2=34.8, B_0=0.47T	[10]

achieved by coating nanoparticles with a variety of different moieties. Here we briefly present two typical and representative methods including coprecipitation method and thermal decomposition method for the synthesis of iron oxides nanoparticles and discuss the commonly used surface modification routes that render these particles compatible with biological environment. For detailed information on the synthesis of such magnetic nanoparticles, excellent review articles are available in the literature [7, 11].

Synthetic Methods

The coprecipitation method is probably the simplest chemical pathway to obtain magnetic nanoparticles. Magnetite (Fe_3O_4) nanoparticles can be prepared from mixture of Fe(II)/Fe(III) aqueous solutions by the addition of a base (ammonia or NaOH) in the presence of stabilizers such as hydrophilic polymers. Dextran is the most commonly used polymer because of its excellent biocompatibility [12, 13]. Several commercial MRI contrast agents based on iron oxide nanoparticles, such as Ferumoxtran-10, Ferumoxide, and Ferucarbotran are all prepared by the coprecipitation method with surface coatings of dextran or its derivates, such as carboxydextran and carboxymethyl dextran. The size and shape of the magnetic iron oxide nanoparticles prepared by coprecipitation method can be tuned by adjusting the nature of the salts (perchlorates, chlorides, sulfates, and nitrates), the Fe^{2+}/Fe^{3+} ratio, the pH value, the reaction temperature, and ionic strength of the reaction media [11]. The coprecipitation technique is the most widely used method and the main advantage is that a large amount of nanoparticles can be synthesized easily. However, the control of particle size distribution is limited because particles prepared by coprecipitation are polydisperse.

Magnetic nanoparticles with a high level of size monodispersity and shape control can be obtained by high-temperature decomposition of iron organic precursors, such as $Fe(CO)_5$, $Fe(acac)_3$, or $Fe(oleate)_3$ in high-boiling organic solvents containing stabilizing surfactants. Sun *et al*. have described the high-temperature decomposition of iron (III) acetylacetonate ($Fe(acac)_3$) in the presence of 1,2-hexadecanediol, oleic acid and oleylamine in phenol ether to obtain monodisperse magnetite nanoparticles with diameters ranging from 3 to 20 nm [14]. For large-scale synthesis of monodisperse nanocrystals, Hyeon *et al.* reported the decomposition of iron oleate complex in various solvents with different boiling points, such as 1-hexadecene, octyl ether, 1-

octadecene, 1-eicosene, or trioctylamine, to obtain magnetic nanoparticles with sizes in the range of 5–22 nm. The particle size can be tuned by adjusting the reaction temperature and aging time [15]. Particle size control is extremely important for revealing the size-dependent biological distributions, pharmacokinetics, and elimination pathways. The precise particle size control achieved by the thermal decomposition method provides great opportunities to reveal the size-dependent behavior in a more reliable way, such as the size-dependent cell fate and permeability across cell membranes. Although magnetic nanoparticles with uniform size and high crystallinity can be synthesized from thermal decomposition of metal precursors in organic media, the obtained nanoparticles are hydrophobic, and are not dispersible in aqueous media. Therefore, it is essential to modify the surface of these nanoparticles to endow them with hydrophilic properties, so that they can be used for various biomedical applications.

Surface Modification

In addition to endow nanoparticles with water solubility, surface modification is important for the nanoparticles to be biocompatible and target-specific. For thermal decomposition prepared hydrophobic nanoparticles, it can be accomplished through exchange with water-dispersible ligands or encapsulation with biocompatible shells (Fig. (**1**)).

Nanoparticles prepared in organic solvents are stabilized by surfactants that have their hydrophilic head groups bound to the surface of the nanoparticles and hydrophobic hydrocarbon tails facing the nonpolar organic solvents. The straightforward method for transforming these hydrophobic nanoparticles from organic to aqueous media is to exchange these surfactant capping ligands with bifunctional ligands. The bifunctional ligand is typically composed of a strong binding part to the surface of the nanoparticles and relatively low binding hydrophilic region. Cheon *et al.* reported that hydrophobic capping ligands coated 12 nm Fe_3O_4 nanoparticles can be stabilized by 2,3-dimercaptosuccinic acids (DMSA) bifunctional ligand [16]. The DMSA forms a stable coating through its carboxylic chelate bonding to the nanoparticle surface, and stabilization of the ligand shells is attained through intermolecular disulfide cross-linkages between the ligands under ambient conditions. The remaining free thiol groups of DMSA ligand can be used for the attachment of target specific antibodies. By a similar approach, dopamine based functional molecules was used to displace the hydrophobic ligands on the magnetic iron oxide particles because the bidentate enediol ligands can firmly coordinate with Fe to form a stable chelating complex [17]. However, metal oxide nanoparticles have relatively unreactive surfaces for surface modification compared to other kinds of nanoparticles, such as chalcogenide-based quantum dots and metal nanoparticles because of a very limited number of binding functional groups available for bifunctional ligands.

Amphiphilic polymeric surfactants can form a stable micellar structure on hydrophobic nanoparticles *via* the hydrophobic interaction between hydrophobic tail groups of the surfactants on the particles surfaces and the hydrophobic region of the polymers. Amphiphilic copolymers derivated from polyethylene glycol (PEG) are most widely used due to the nontoxic, nonimmunogenic and protein fouling resistant characteristics of PEG. The outer surface of thus modified nanoparticles is comprised of a dense PEG layer, which render the nanoparticles dispersible and stable in biological media. This strategy, was first used to develop quantum dots, has been successfully extended to magnetic nanoparticles [18]. The functional groups of modified PEG can allow for bioconjugation of various targeting molecules or therapeutic agents on the nanoparticles surface. However, PEG-coated nanoparticles may have limited binding sites available for further fictionalization due to the limited number of functional groups on the nanoparticles' surface. Recently, Nie *et al.* have developed an amphiphilic triblock polymer that has surface reactivity for introducing various or multiple functional groups including the carboxylate group that can be used to cross-link "probe molecules" for biomarker-targeted specific binding [19]. The surface modification with target-oriented molecules will enhance the localization of the imaging probes to specific sites. By incorporation of other advanced features, such as multimodality and therapeutic delivery, the detectability and applicability of magnetic nanoparticles will be further expanded.

MECHANISMS OF CELL LABELING

Recent advances of cell therapy have shown a great potential of stem cells and progenitor cells in regenerative medicine. With SPIO labeling, the distributions, homing and

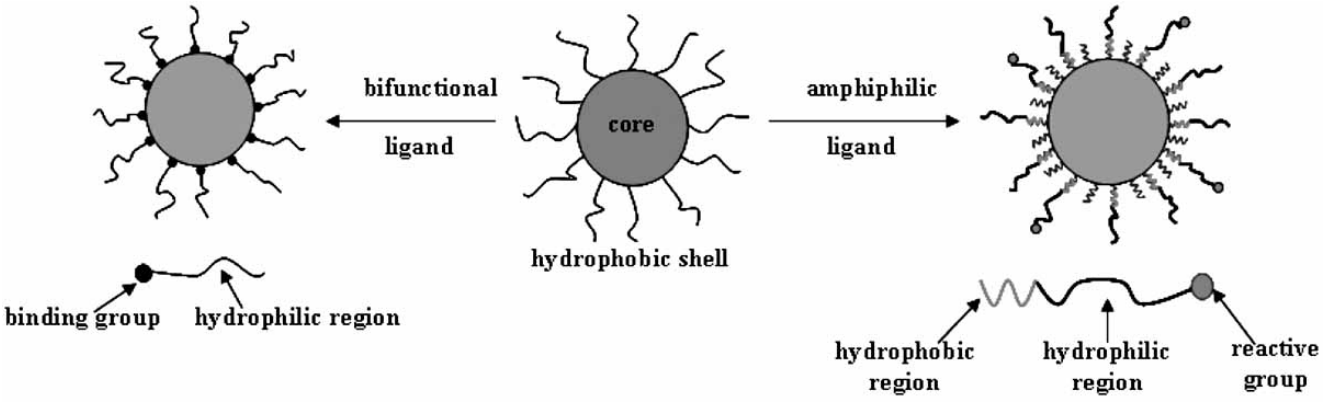

Fig. (1). Surface modification of thermal decomposition synthesized iron oxide nanoparticles by ligand exchange which can give high colloidal stability in aqueous biofluids or capability to couple with other ligands.

engraftment of implanted cells can be successfully detected using MR [20].

Labeling Approaches

There are a large range of approaches that had been used for cell labeling with experimentally and clinically approved SPIOs. These approaches can be classified into three fundamental categories, including *in vitro* cell labeling (e.g. with transfection agents, endocytosis, electroporation, magnetofection), *in vivo* cell labeling by reticuloendothelial system (RES) through systemic application, receptor-mediated binding and internalization of SPIOs by targeted cells (e.g. targeted labeling and imaging). The appropriate labeling approach is used depending on the specific purpose.

A recent study demonstrated a novel approach in which cells can accumulate contrast agents by genetically modification with an MRI reporter gene encoding metalloproteins. This reporter can make superparamagnetism as the cell sequesters endogenous iron from the organism. *In vitro* studies showed that ferritin-transduced cells had enhanced iron loading as assessed by iron uptake and NMR relaxation rates. The similar results were also achieved in animal studies by injection of the vector-encoded reporter into mouse striatum [21].

Internalization of SPIOs

Endocytosis is the process by which cells absorb material through engulfing material with cell membrane. This process plays a crucial role in cell labeling with SPIOs. This process can be mainly subdivided into phagocytosis, pinocytosis and receptor-mediated endocytosis which are depended on the size of the vesicles formed and the cellular machinery involved. By systemic administration, SPIOs (e.g. Ferumoxides, the contrast agent used for liver imaging clinically) are mainly recognized and taken up by macrophages as extraneous material through phagocytosis and accumulate in liver, spleen, bone marrow and lymph nodes [22].

For *in vitro* cell labeling, SPIOs always need to have diameters no more than 150nm since they are internalized mainly by pinocytosis which with respect to the uptake of solutes and single molecules such as proteins or small size particles. However, both phagocytosis and pinocytosis are non-receptor-mediated forms of endocytosis and result in non-specific internalization of particles. As SPIOs are negatively charged in physiological pH conditions, cationic transfection agents are always used for forming a positive compounds couple with negatively charged SPIOs which can promote the cell internalization. In order to achieve more specific MR imaging of particular target, development of targeted contrast agents is another most promising approach. Recently, targeted SPIOs are chemically modified by conjugation with targeting agents such as monoclonal antibodies, peptides, or small molecules antibodies. By systemic administration, these targeted SPIOs can accumulate specifically in certain cells or tissues and generate enhanced contrast for MR detection. In this approach, internalization of contrast agents is achieved mainly by receptor-mediated endocytosis. When proteins or other trigger particles lock into receptors or ligands in the plasma membrane of the cell, the cytoplasm membrane will fold inward to form coated pits and then the particle is engulfed [23].

By internalization of cells, SPIOs are always localized in endosome, which are still separated from the cytoplasm of the cell by a membrane. Most of SPIOs utilizing in clinical or pre-clinical tests are coated with a biodegradable surface which will always degrade by enzymes of cells [7]. Iron cores will integrate into body iron stores and then incorporate into erythrocyte hemoglobin [3, 24, 25].

Size Effect

Size is an important factor for SPIOs in MR contrast-enhancement effect. In nanoscale regime, surface spins of SPIOs tend to be slightly tilted to form a magnetically disordered spin-glass-like surface layer which influence significantly on their magnetic moments and MR contrast-enhancement effects. This effect is size dependent and there is a linear relationship between size and magnetization values [16].

In addition to particle composition, the hydrodynamic size of SPIOs also plays an important role in determining the biological properties, such as blood half-lives, absorption, distribution, metabolism and excretion. Particles such as SPIOs which have a diameter more than 200nm are taken up significantly by spleen. With a size less than 5-6 nm, particles are rapidly removed by extravasation and renal clearance [26]. The blood half-lives of different type of SPIOs in human vary from 1 h to 36 h [3]. In comparison with large SPIOs, the lower uptake by RES make small SPIOs have a long blood half-lives which could facilitate the accumulation of SPIOs in specific sites and achieve an adequate level of iron load. It has been reported that the size of SPIO particles is related to the cell labeling efficiency. Ferucarbotran with smaller size had higher efficiency than Ferumoxides for the labeling of adipose tissue derived stem cells (ADSCs) [27]. We also identified the labeling efficiency of three SPIOs (10, 30, 50nm in diameter, respectively) with the same polymer coatings (about 10nm) for the labeling of dermis-derived multipotential stem cells (DMCs). The Results showed that the smallest particles had a highest labeling efficiency compared with other two (Fig. **2**) [28]. Even though the magnetic moment of SPIOs is size dependent [16], the large amount of small size SPIOs in cells can retrieve this situation and generate a lower signal in MRI.

Surface Ligand Effect

Surface coatings are used for preventing the destabilization and agglomeration of SPIOs. These coating materials include surfactants or polymers, organic and inorganic molecules. Without a surface protection, iron oxide nanoparticles can produce a nanoparticle-specific cytotoxicity on human mesothelioma and rodent fibroblast cell line [29]. The hydrodynamic size of SPIOs which plays a critical role in biological application can vary widely depending on the type of coating and surface modification method. SPIOs with different polymer coatings or even minor surface modifications can result in different stability, uptake and toxicity [30].

Independent of particle size, charge also affects the labeling efficiency. The uptake of SPIOs may slow by negative charges because of the negative charge of cell membrane. *In vitro*, a zeta potential close to zero can decrease the endocytosis of iron oxide nanoparticles significantly. However, both

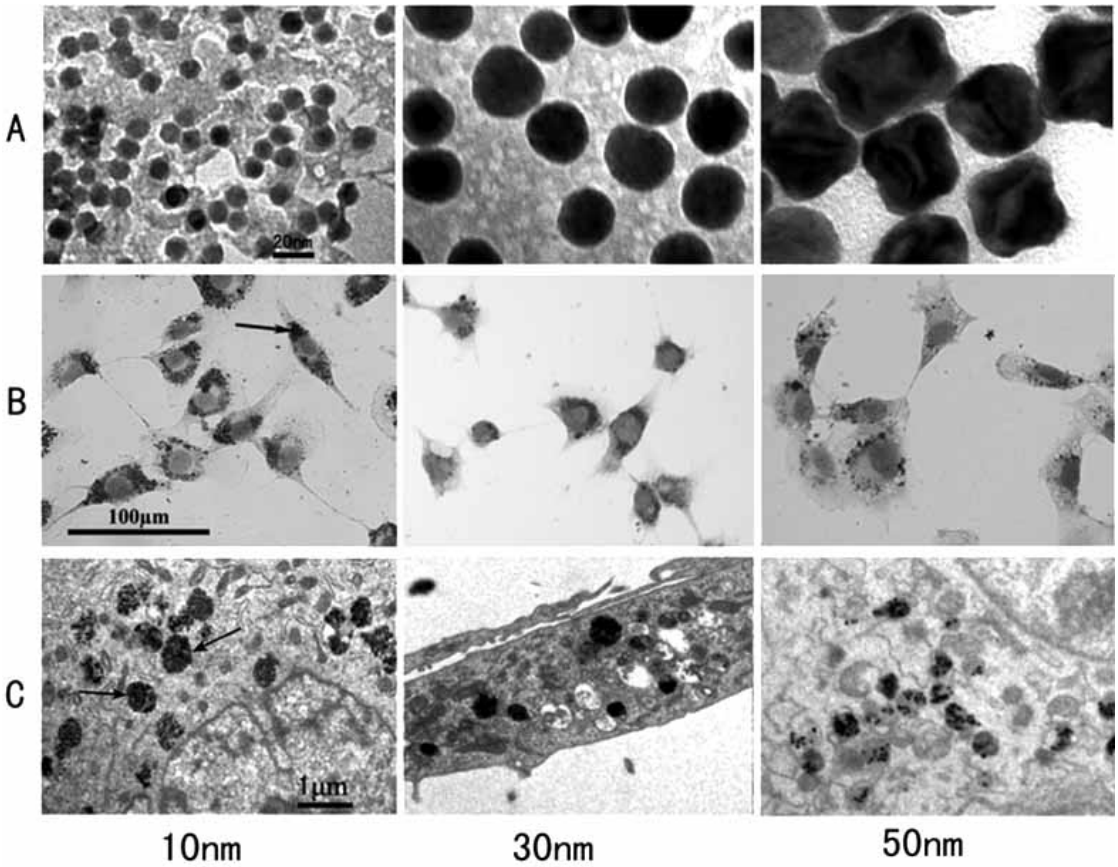

Fig. (2). A. Transmission electron microscopy (TEM) images of SPIOs with the diameters of 10, 30 and 50nm, respectively. B. *In vitro* Prussian blue assessment of iron uptake by dermis-derived multipotent stem cells (DMCs). Photomicrographs show positive Prussian blue staining of DMCs incubated with different SPIOs for 24 h at a concentration of 25μgFe/ml. C. TEM images of DMCs pretagged with SPIOs. The localization of iron oxide particles containing organelles (black deposits) can be distinguished by their morphology from other contrasted intracellular organelles. The particle clusters (indicated as arrows) can be found in the endosomes.

negative or positive surface charge can increase the phagocytosis of SPIOs and the higher surface charge will shorten the blood half-lives of particles in circulation. To enhance the internalization of SPIOs, a serial of cationic agents such as protamine sulfate, lipofectamine and poly-L-lysine (PLL) are used as transfection agents for cell labeling *in vitro*. These positive charged molecules usually bind to anionic cell membrane and increase the transfection efficiency through promoting the binding of SPIOs and membrane receptor [31]. Following the development of synthesis technique, SPIOs with appropriate positive surface ligands can be effectively transported inside cells. A recent study showed that by conjugation of SPIOs with a non-toxic protein transduction domain (PTD), the labeling efficiency of these particles are higher than SPIOs [32].

As described above, the cell labeling efficiency is dependent on the particle hydrodynamic size, the nature and charge of the surface coatings. Long term cell tracking and imaging request high labeling efficiency and magnetism of SPIOs. To achieve this goal, the elucidation of the relationships between the physicochemical properties and pharmacokinetics of SPIOs and the improved surface modifications to obtain higher superparamagnetism, permeability and stability to generate sufficient signal in MR are needed.

APPLICATIONS IN CELL LABELING AND TRACKING

As negative MR contrast agents, SPIOs were first used in liver imaging. After systemic administration, SPIO particles are rapidly taken up by hepatic specialized macrophages, Kupffer cells, resulting in a local signal loss on MR images. A recent study showed that after systemic administration of SPIOs in rats, more than 90% of iron accumulated in liver and spleen [33]. Since Kupffer cells are exclusively located in the healthy hepatic parenchyma, SPIOs can increase the contrast between normal tissues and tumors which are devoid of Kupffer cells [34]. The majority of nonspecific cellular labeling has so far involved macrophages which are important markers of local inflammation. As a result, a serial of ideal methods for inflammatory diseases detection by MRI has been developed due to the infiltration of SPIOs loaded macrophages. Macrophages with a certain amount of SPIOs will migrate into the injury site and then can be monitored by MRI [35]. Recently, SPIOs were also used in early detection of atherosclerosis since inflammation plays a pivotal role in atherosclerotic plaque growth and instability [36,37].

Cell therapy has been used in the management of numerous diseases such as neurologic diseases [38-40], cardiovascular diseases [41], renal and hepatic diseases [42]. Most

cells used in cell therapy are non-phagocytes and need to be pre-tagged with SPIOs before implantation. In cerebral disease models, prior studies showed that the migration of SPIOs labeled cells could across the brain from the implantation site to the injury or hemorrhage site [38-40]. Song *et al*. transplanted SPIOs labeled neural stem cells (NSCs) into the distal region of injured spinal cord, the cell migration along the spinal cord to the site of lesion was detected by MRI 3 weeks later [43]. By systemic administration of SPIOs labeled stem cells, such as hematopoietic progenitor cells or mesenchymal stem cells (MSCs), the lesion site always present a signal void in MRI due to the accumulation of labeled cells [44, 45]. Since a serial of successful results have been achieved in animal studies, the early-phase clinical investigations using noninvasive MRI to monitor cellular migration in patients have been performed. Recently, Zhu *et al*. used the clinically approved Ferumoxides to label human neural stem cells in culture and then re-injected these labeled cells to a brain traumatic patient [1]. Under a 3T clinical MR system, subsequent migration of the implanted cells from the primary injection sites to the border of the damaged tissues was monitored successfully.

Recent studies have demonstrated the feasibility to detect a small number of cells (from 120 to 1000 cells/mm^3) by MRI [46-49]. Recent studies even showed that single cell labeled with SPIO nanoparticles could be detected with a 1.5 T clinical scanner [50] and femtomole quantities of SPIOs could be detected under typical micro-imaging conditions [51]. Regarding the long term tracking, Farrell *et al*. reported that Ferumoxides labeled human MSCs which were seeded onto collagen-GAG scaffolds and transplanted subcutaneously into the nude mice could be detected *in vivo* for 7 weeks [52]. The even longer tracking term of 18 weeks was also demonstrated by using Ferumoxides to label human central nervous system stem cells derived neurosphere cells (hCNS-SCns) [53].

However, there are still several critical issues that need to be addressed. The long term tracking of SPIO-labeled stem cells will be restricted by cell division since the cellular iron content will decrease during cell division. The signal change of MRI dependent on local concentration of SPIOs but not the labeled cell number. The more accurate quantification of the number of SPIOs labeled cells is limited by cell proliferation. In addition, the uptake of SPIOs which released from implanted cells by non-stem cells around the transplantation site also affects the detection and quantification of the implanted cells. However, a recent study showed that the internalization of released SPIOs by host cells may be limited in just a pretty low level. By injection of enhanced green fluorescent proteins (eGFP) and SPIOs double labeled adipose-derived stem cells (ADSCs) into the infarction region of rat heart for 4 weeks, most SPIOs containing ADSCs expressed eGFP indicating that signal voids of MRI mainly reflect the living transplanted cells [54]. The similar results were also observed in other studies [55, 56]. In most cases, MRI studies are always conducted with a 1.5/3.0 T MRI unit. When the content of SPIOs in labeled cells decreased to a low level, the difference between adjacent tissue and labeled cells will not be detected by these facilities. Although this limitation can be improved by increase the labeling efficiency and enhance the field strength of MRI, the potential hazards of more iron loading and strong magnetic fields are still need to be evaluated [51]. In addition, stem cells can differentiate into many cell types in different environments and it is difficult to determine the cell state only by signal loss of MRI.

SAFETY CONCERNS OF SPIO IN BIOMEDICAL APPLICATIONS

Toxicity of SPIOs is dependent on several factors such as iron dose, hydrodynamic size, surface coatings, charge and the way of administration. Different sizes of SPIOs have different blood half-lives and distribution. In addition to size, nature of coatings also plays a critical role in determining the characteristics and distribution.

In animal studies, after systemic administration of Ferumoxides, particles are mainly uptaken by liver and spleen in a couple of hours, and only minimal amounts of SPIOs locate in other tissues such as kidney, lung, and brain. Iron was incorporated into hemoglobin of erythrocytes time dependently and no acute or subacute toxicities were detected in the rats and dogs at 3000 μmol Fe/kg, which is 150 times of the dose proposed for liver imaging [57]. In human studies, the adverse events of ferumoxtran-10 or Feridex IV are noted as slight and short in duration [22, 58]. The most common reactions are headache, back pain, vasodilatation and urticaria. Most adverse events begin within 1 hour and resolve within 24 hours after administration, while only a few cases need symptomatic treatment. The exact physiologic mechanism of these adverse events is not well understood, but is hypothesized to be occlusion of microvascular structures of the paraspinal muscles, renal artery spasm, or allergic reaction [58].

Many studies showed that SPIOs had a minimal impact on cell viabilities and functions even at high iron concentrations [59-61]. However, other studies have shown some adverse effects of SPIOs in cells (Table **2**). In general, cytotoxicity of different SPIOs depends on their iron content, surface coatings, transfection agents used and incubation duration. The increase of cellular iron content might lead to an increase of the reactive oxygen species (ROS) and result in damage of DNA and cellular membrane [62-64]. However, ferritin synthesis is stimulated by increased iron content and the free iron uptake by ferritin molecules will reduce this toxic effect [63]. The surface ligands also play an critical role in cytotoxicity. A synthetic iron oxide particle with amines surface exhibited adverse cell influence at 10 μg/ml after 4 hours incubation in immortalized human T cells. When the amines were completely blocked, cell death was reduced to a negligible level. This cell death was likely attributable to extremely high driving force for cell internalization imparted by positive SPIO surface charge. This cytotoxicity was also reduced by shorten the labeling duration [65]. As most SPIOs present anionic surface charges, transfection agents are usually used to promote the labeling efficiency. PLL and Lipofectamine2000 are widely used in many studies, however, they have cytotoxicity at low concentrations and are not approved for clinical use by the Food and Drug Administration (FDA) [66]. Regarding the polymer coatings, several studies showed that the toxicity of polymers could be

Table 2. Potential Cytotoxic Effects of SPIOs

Particle size	Surface coatings	Cell type	Transfection agents	Does of SPIO	Exposure duration	Results	Refs.
20nm (hydrodynamic diameter)	1-hydroxyethylidene-1.1-bisphosphonic acid (HEDP)	Rat MSCs	Fugene (1μl/ml)	25, 50 and 100ugFe /ml	24 hours	No affect on cell viability with 25 or 50 μg iron/ml, whereas decrease with 100 μg iron/ml.	[78]
150nm (hydrodynamic diameter)	Dextran	Human umbilical vein endothelial cells (HUVECs)	Lipofectamine 2000 (2μg/ml)	800ugFe /150m^2 dish in a total volume of 15ml	24 hours	Significant decrease of mitochondrial membrane potential at doses ≥200μgFe/ml and cell death at 800μgFe/ml	[79]
5-12nm (by TEM)	Dimercaptosuccinic acid (DMSA)	Rat pheochromocytoma cells (PC12)	None	15, 1.5 and 150 mM	24 hours	Dose dependent diminution viability and capacity to form neurites in response to nerve growth factor.	[80]
50nm (hydrodynamic diameter)	Carboxydextran	Murine macrophages	None	1, 10 and 100μg Fe/ml	24 hours	Dose–dependent increase of NO production and decrease of phagocytic function,	[81]
30 and 47 nm	None available	Rat liver derived cells	None	10, 50, 100 and 250μg Fe/ml	24 hours	No affect on cell viability up to the concentration of 100 μg iron/ml, but a significant cytotoxic effect at 250 μg iron/ml.	[82]
60nm (hydrodynamic diameter)	Carboxydextran	Rat MSCs	None	200μg Fe/ml	4 and 15 hours	Up-regulation of transferrin receptor (CD70) expression	[83]
50nm (hydrodynamic diameter)	Carboxydextran	Human MSCs	None	10, 30, 100 and 300μg Fe/ml	1 hour	Increased cell viability at doses ≤300μgFe/ml	[84]
Various from 4 to 86nm by TEM	Polyvinyl Alcohol (PVA)	Mouse connective tissue cells	None	0.2, 1, 5, and 20 mM	2h ours	Increased cell viability related to the hydrodynamic size of the particles.	[85]
20-40nm and 100 -500nm by TEM	None available	Human alveolar type II-like epithelial cells (A549)	None	40μg Fe /cm^2	18 hours	No significant difference between the two particles.	[86]
60nm (hydrodynamic diameter)	Carboxydextran	Human MSCs	Cationic amphiphile molecule (Pulsin™)	60 and 200μg Fe/ml	4 hours	Significant reduction of colony-formation ability and transient decrease of migration capacity by Pulsin™ compound with SPIOs.	[87]

reduced by conjugation with SPIOs. Polyethylenimine (PEI) was thought to has cytotoxicity by non-specific interactions with cell membranes. Interestingly, when conjugated onto SPIOs (~10 nm), the cytotoxicity of PEI significantly reduced. The less toxicity of SPIO-PEI might be due to the restriction of the polymer mobility and thus limited the non-specific interactions with the cell membranes [67].

CONCLUDING REMARKS

An ideal MRI imaging modality for cell labeling and tracking should have the following properties including biocompatibility, nontoxicity, no genetic modification or interference to cell behaviors with high magnetism and iron load. Given the inherent limitations of currently available imaging technologies, there is an urgent need to develop methods and strategies to produce improved imaging probes fulfilling above criteria. Recent progresses have been made on the development of some metal alloys magnetic nanoparticles such as FeCo and FePt to generate higher magnetic moments. The application of higher field clinical scanners also will allow increased sensitivity for labeled therapeutic cell detection. However, the potential hazards of more iron uptake and strong magnetic fields are needed to be evaluated further [51]. Recent advances also have demonstrated the feasibility of developing magnetic nanoparticles with multimodality for tumor imaging and therapy [68, 69]. Such examples include probes in which SPIO nanoparticles are coupled with other functional agents (e.g. targeted molecules, alternative imaging probes and therapeutic drugs). This approach is expected to lead to development of novel multifunctional and more advantageous probes for MRI imaging.

ACKNOWLEDGEMENTS

This work was supported by State Key Basic Research Development Programs (NO. 2005CB522605 and 2010529403), Chongqing Municipal Natural Science Foun-

dation Programs (CSTC2009BA5043 and 2008BB5023)., National Natural Science Foundation Programs (NFSC30870966 and 30571893), and State Education Ministry Programs (FANEDD200777 and IRT0712). This research is also funded by intramural grants from the Third Military Medical University and State Key Laboratory of Trauma, Burns and Combined Injury (SKLZZ200810).

ABBREVIATIONS

ADSC = Adipose tissue derived stem cell

BPEI = Branched polyethylenimine

DMC = Dermis-derived multipotential stem cell

DMSA = Dimercaptosuccinic acid

HCNS-SCN = Human central nervous system Stem Cells Derived Neurosphere Cell

HUVECs = Human umbilical vein endothelial cells

IC50 = Half maximal inhibitory concentration

MION = Monocrystalline iron oxide nanoparticles

MRI = Magnetic resonance imaging

MSC = Mesenchymal stem cell

NMR = Nuclear magnetic resonance

NSC = Neural stem cell

PEG = Polyethylene glycol

PC12 = Pheochromocytoma cells

PEI = Polyethylenimine

PLL = Poly-L-lysine

PTD = Protein transduction domain

RES = Reticulo endothelial system

ROS = Reactive oxygen species

SPIO = Superparamagnetic iron oxide

SSPIO = Standard superparamagnetic iron oxide

TEM = Transmission electron microscopy

USPIO = Ultra-small superparamagnetic iron oxide

VSOP = Very small superparamagnetic iron oxide

REFERENCES

[1] Zhu, J.; Zhou, L.; Xing, W. F. Tracking neural stem cells in patients with brain trauma. *N. Engl. J. Med.*, **2006**, *355*, 2376-2378.

[2] Wang, X.; Yang, L.; Chen, Z.G.; Shin, D.M. Application of nanotechnology in cancer therapy and imaging. *CA Cancer J Clin.*, **2008**, *58*, 97-110.

[3] Corot, C.; Robert, P.; Idee, J.M.; Port, M. Recent advances in iron oxide nanocrystal technology for medical imaging. *Adv. Drug Deliv. Rev.*, **2006**, *58*, 1471-1504.

[4] Jeong, U.; Teng, X.W.; Wang, Y.; Yang, H.; Xia, Y.N. Superparamagnetic colloids: controlled synthesis and niche applications *Adv. Mater.*, **2007**, *19*, 33-60.

[5] Jun, Y.W.; Seo, J.W.; Cheon, J. Nanoscaling laws of magnetic nanoparticles and their applicabilities in biomedical sciences. *Acc. Chem. Res.*, **2008**, *41*, 179-189.

[6] Tanimoto, A.; Kuribayashi, S. Application of superparamagnetic iron oxide to imaging of hepatocellular carcinoma. *Eur. J. Radiol.*, **2006**, *58*, 200-2016.

[7] Jun, Y.W.; Lee, J.H.; Cheon, J. Chemical design of nanoparticle probes for high-performance magnetic resonance imaging. *Angew. Chem. Int. Ed. Engl.*, **2008**, *47*, 5122-5135.

[8] Thorek, D.L.; Chen, A.K.; Czupryna, J.; Tsourkas, A. Superparamagnetic iron oxide nanoparticle probes for molecular imaging. *Ann. Biomed. Eng.*, **2006**, *34*, 23-38.

[9] Taupitz, M.; Wagner, S.; Schnorr, J.; Kravec, I.; Pilgrimm, H.; Bergmann-Fritsch, H.; Hamm, B. Phase I clinical evaluation of citrate-coated monocrystalline very small superparamagnetic iron oxide particles as a new contrast medium for magnetic resonance imaging. *Invest. Radiol.*, **2004**, *39*, 394-405.

[10] Shen, T.; Weissleder, R.; Papisov, M.; Bogdanov, A., Jr.; Brady, T.J. Monocrystalline iron oxide nanocompounds (MION): physicochemical properties. *Magn. Reson. Med.*, **1993**, *29*, 599-604.

[11] Laurent, S.; Forge, D.; Port, M.; Roch, A.; Robic, C.; Vander Elst, L.; Muller, R.N. Magnetic iron oxide nanoparticles: synthesis, stabilization, vectorization, physicochemical characterizations, and biological applications. *Chem. Rev.*, **2008**, *108*, 2064-2110.

[12] Molday, R.M., D. Immunospecific ferromagnetic iron-dextran reagents for the labeling and magnetic separation of cells. *J. Immunol. Methods*, **1982**, *52*, 353-367.

[13] Berry, C.C.; Wells, S.; Charles, S.; Aitchison, G.; Curtis, A.S. Cell response to dextran-derivatised iron oxide nanoparticles post internalisation. *Biomaterials*, **2004**, *25*, 5405-5413.

[14] Sun, S.; Zeng, H.; Robinson, D.B.; Raoux, S.; Rice, P.M.; Wang, S.X.; Li, G. Monodisperse MFe2O4 (M = Fe, Co, Mn) nanoparticles. *J. Am. Chem. Soc.*, **2004**, *126*, 273-279.

[15] Park, J.; An, K.; Hwang, Y.; Park, J.G.; Noh, H.J.; Kim, J.Y.; Park, J.H.; Hwang, N.M.; Hyeon, T. Ultra-large-scale syntheses of monodisperse nanocrystals. *Nat. Mater.*, **2004**, *3*, 891-895.

[16] Jun, Y.W.; Huh, Y.M.; Choi, J.S.; Lee, J.H.; Song, H.T.; Kim, S.; Yoon, S.; Kim, K.S.; Shin, J.S.; Suh, J.S.; Cheon, J. Nanoscale size effect of magnetic nanocrystals and their utilization for cancer diagnosis via magnetic resonance imaging. *J. Am. Chem. Soc.*, **2005**, *127*, 5732-5733.

[17] Xu, C.; Xu, K.; Gu, H.; Zheng, R.; Liu, H.; Zhang, X.; Guo, Z.; Xu, B. Dopamine as a robust anchor to immobilize functional molecules on the iron oxide shell of magnetic nanoparticles. *J. Am. Chem. Soc.*, **2004**, *126*, 9938-9939.

[18] Dubertret, B.; Skourides, P.; Norris, D.J.; Noireaux, V.; Brivanlou, A.H.; Libchaber, A. *In vivo* imaging of quantum dots encapsulated in phospholipid micelles. *Science*, **2002**, *298*, 1759-1762.

[19] Gao, X.; Cui, Y.; Levenson, R.M.; Chung, L.W.; Nie, S. *In vivo* cancer targeting and imaging with semiconductor quantum dots. *Nat. Biotechnol.*, **2004**, *22*, 969-976.

[20] Hoehn, M.; Wiedermann, D.; Justicia, C.; Ramos-Cabrer, P.; Kruttwig, K.; Farr, T.; Himmelreich, U. Cell tracking using magnetic resonance imaging. *J. Physiol.*, **2007**, *584*, 25-30.

[21] Genove, G.; DeMarco, U.; Xu, H.; Goins, W.F.; Ahrens, E.T. A new transgene reporter for in vivo magnetic resonance imaging. *Nat. Med.*, **2005**, *11*, 450-454.

[22] Ros, P.R.; Freeny, P.C.; Harms, S.E.; Seltzer, S.E.; Davis, P.L.; Chan, T.W.; Stillman, A.E.; Muroff, L.R.; Runge, V.M.; Nissenbaum, M.A. Hepatic MR imaging with ferumoxides: a multicenter clinical trial of the safety and efficacy in the detection of focal hepatic lesions. *Radiology*, **1995**, *196*, 481-488.

[23] Peng, X.H.; Qian, X.; Mao, H.; Wang, A.Y.; Chen, Z.G.; Nie, S.; Shin, D.M. Targeted magnetic iron oxide nanoparticles for tumor imaging and therapy. *Int. J. Nanomed.*, **2008**, *3*, 311-321.

[24] Schulze, E.; Ferrucci, J.T., Jr.; Poss, K.; Lapointe, L.; Bogdanova, A.; Weissleder, R. Cellular uptake and trafficking of a prototypical magnetic iron oxide label *in vitro*. *Invest. Radiol.*, **1995**, *30*, 604-610.

[25] Anzai, Y. Superparamagnetic iron oxide nanoparticles: nodal metastases and beyond. *Top. Magn. Reson. Imaging*, **2004**, *15*, 103-111.

[26] Choi, H.S.; Liu, W.; Misra, P.; Tanaka, E.; Zimmer, J.P.; Itty, I. B.; Bawendi, M.G.; Frangioni, J.V. Renal clearance of quantum dots. *Nat. Biotechnol.*, **2007**, *25*, 1165-1170.

[27] Zhang, C.; Shi, CM. Superparamagnetic iron oxide nanoparticles for *in vivo* stem cell tracking. *Exp. Hematol.*, **2009**, *37*(Suppl 1), 102.

[28] Park, B.H.; Jung, J., C.; Lee, G.H.; Kim, T.J.; Lee, Y.J.; Kim, J.Y.; Kim, Y.W.; Jeong, J.H.; Chang, Y. Comparison of labeling efficiency of different magneticnanoparticles into stem cell. *Colloids Surf. A: Physicochem. Eng. Aspects.*, **2008**, *313-314*, 145-149.

[29] Brunner, T.J.; Wick, P.; Manser, P.; Spohn, P.; Grass, R.N.; Limbach, L.K.; Bruinink, A.; Stark, W.J. *In vitro* cytotoxicity of oxide nanoparticles: comparison to asbestos, silica, and the effect of particle solubility. *Environ. Sci. Technol.*, **2006**, *40*, 4374-4381.

[30] Petri-Fink, A.; Steitz, B.; Finka, A.; Salaklang, J.; Hofmann, H. Effect of cell media on polymer coated superparamagnetic iron oxide nanoparticles (SPIONs): colloidal stability, cytotoxicity, and cellular uptake studies. *Eur. J. Pharm. Biopharm.*, **2008**, *68*, 129-137.

[31] Bulte, J.W.; Douglas, T.; Witwer, B.; Zhang, S.C.; Strable, E.; Lewis, B.K.; Zywicke, H.; Miller, B.; van Gelderen, P.; Moskowitz, B.M.; Duncan, I.D.; Frank, J.A. Magnetodendrimers allow endosomal magnetic labeling and in vivo tracking of stem cells. *Nat. Biotechnol.*, **2001**, *19*, 1141-1147.

[32] Suh, J.S.; Lee, J.Y.; Choi, Y.S.; Yu, F.; Yang, V.; Lee, S.J.; Chung, C.P.; Park, Y.J. Efficient labeling of mesenchymal stem cells using cell permeable magnetic nanoparticles. *Biochem. Biophys. Res. Commun.*, **2009**, *379*, 669-675.

[33] Ma, H.L.; Xu, Y.F.; Qi, X.R.; Maitani, Y.; Nagai, T. Superparamagnetic iron oxide nanoparticles stabilized by alginate: pharmacokinetics, tissue distribution, and applications in detecting liver cancers. *Int. J. Pharm.*, **2008**, *354*, 217-226.

[34] Kim, S.H.; Lee, W.J.; Lim, H.K.; Park, C.K. SPIO-enhanced MRI findings of well-differentiated hepatocellular carcinomas: correlation with MDCT findings. *Korean J. Radiol.*, **2009**, *10*, 112-20.

[35] Bendszus, M.; Stoll, G. Caught in the act: *in vivo* mapping of macrophage infiltration in nerve injury by magnetic resonance imaging. *J. Neurosci.*, **2003**, *23*, 10892-10896.

[36] Ruehm, S.G.; Corot, C.; Vogt, P.; Kolb, S.; Debatin, J.F. Magnetic resonance imaging of atherosclerotic plaque with ultrasmall superparamagnetic particles of iron oxide in hyperlipidemic rabbits. *Circulation*, **2001**, *103*, 415-422.

[37] Kooi, M.E.; Cappendijk, V.C.; Cleutjens, K.B.; Kessels, A.G.; Kitslaar, P.J.; Borgers, M.; Frederik, P.M.; Daemen, M.J.; van Engelshoven, J.M. Accumulation of ultrasmall superparamagnetic particles of iron oxide in human atherosclerotic plaques can be detected by in vivo magnetic resonance imaging. *Circulation.*, **2003**, *107*, 2453-2458.

[38] Hoehn, M.; Wiedermann, D.; Justicia, C.; Ramos-Cabrer, P.; Kruttwig, K.; Farr, T.; Himmelreich, U. Cell tracking using magnetic resonance imaging. *J. Physiol.*, **2007**, *584*, 25-30. [39] Chang, N.K.; Jeong, Y.Y.; Park, J.S.; Jeong, H.S.; Jang, S.; Jang, M.J.; Lee, J.H.; Shin, S.S.; Yoon, W.; Chung, T.W.; Kang, H.K. Tracking of neural stem cells in rats with intracerebral hemorrhage by the use of 3T MRI. *Korean J. Radiol.*, **2008**, *9*, 196-204.

[40] Guzman, R.; Bliss, T.; De Los Angeles, A.; Moseley, M.; Palmer, T.; Steinberg, G. Neural progenitor cells transplanted into the uninjured brain undergo targeted migration after stroke onset. *J. Neurosci. Res.*, **2008**, *86*, 873-882.

[41] Arai, T.; Kofidis, T.; Bulte, J.W.; de Bruin, J.; Venook, R.D.; Berry, G.J.; McConnell, M.V.; Quertermous, T.; Robbins, R.C.; Yang, P.C. Dual *in vivo* magnetic resonance evaluation of magnetically labeled mouse embryonic stem cells and cardiac function at 1.5 t. *Magn. Reson. Med.*, **2006**, *55*, 203-209.

[42] Bos, C.; Delmas, Y.; Desmouliere, A.; Solanilla, A.; Hauger, O.; Grosset, C.; Dubus, I.; Ivanovic, Z.; Rosenbaum, J.; Charbord, P.; Combe, C.; Bulte, J.W.; Moonen, C.T.; Ripoche, J.; Grenier, N. *In vivo* MR imaging of intravascularly injected magnetically labeled mesenchymal stem cells in rat kidney and liver. *Radiology*, **2004**, *233*, 781-789.

[43] Song, H.T.; Choi, J.S.; Huh, Y.M.; Kim, S.; Jun, Y.W.; Suh, J.S.; Cheon, J. Surface modulation of magnetic nanocrystals in the development of highly efficient magnetic resonance probes for intracellular labeling. *J. Am. Chem. Soc.*, **2005**, *127*, 9992-9993.

[44] Qiu, B.; Yang, X. Molecular MRI of hematopoietic stem-progenitor cells: in vivo monitoring of gene therapy and atherosclerosis. *Nat. Clin. Pract. Cardiovasc. Med.*, **2008**, *5*, 396-404.

[45] Gao, F.; Kar, S.; Zhang, J.; Qiu, B.; Walczak, P.; Larabi, M.; Xue, R.; Frost, E.; Qian, Z.; Bulte, J.W.; Yang, X. MRI of intravenously injected bone marrow cells homing to the site of injured arteries. *NMR. Biomed.*, **2007**, *20*, 673-681.

[46] Verdijk, P.; Scheenen, T.W.; Lesterhuis, W.J.; Gambarota, G.; Veltien, A.A.; Walczak, P.; Scharenborg, N.M.; Bulte, J.W.; Punt, C.J.; Heerschap, A.; Figdor, C.G.; de Vries, I.J. Sensitivity of magnetic resonance imaging of dendritic cells for in vivo tracking of cellular cancer vaccines. *Int. J. Cancer*, **2007**, *120*, 978-984.

[47] Hoehn, M.; Kustermann, E.; Blunk, J.; Wiedermann, D.; Trapp, T.; Wecker, S.; Focking, M.; Arnold, H.; Hescheler, J.; Fleischmann, B.K.; Schwindt, W.; Buhrle, C. Monitoring of implanted stem cell migration in vivo: a highly resolved in vivo magnetic resonance imaging investigation of experimental stroke in rat. *Proc. Natl. Acad. Sci. USA*, **2002**, *99*, 16267-16272.

[48] Magnitsky, S.; Watson, D.J.; Walton, R.M.; Pickup, S.; Bulte, J.W.; Wolfe, J.H.; Poptani, H. *In vivo* and *ex vivo* MRI detection of localized and disseminated neural stem cell grafts in the mouse brain. *Neuroimage*, **2005**, *26*, 744-754.

[49] Dahnke, H.; Schaeffter, T. Limits of detection of SPIO at 3.0 T using T2 relaxometry. *Magn. Reson. Med.*, **2005**, *53*, 1202-1206.

[50] Foster-Gareau, P.; Heyn, C.; Alejski, A.; Rutt, B.K. Imaging single mammalian cells with a 1.5 T clinical MRI scanner. *Magn. Reson. Med.*, **2003**, *49*, 968-971.

[51] Heyn, C.; Ronald, J.A.; Mackenzie, L.T.; MacDonald, I.C.; Chambers, A.F.; Rutt, B.K.; Foster, P.J. *In vivo* magnetic resonance imaging of single cells in mouse brain with optical validation. *Magn. Reson. Med.*, **2006**, *55*, 23-29.

[52] Farrell, E.; Wielopolski, P.; Pavljasevic, P.; van Tiel, S.; Jahr, H.; Verhaar, J.; Weinans, H.; Krestin, G.; O'Brien, F.J.; van Osch, G.; Bernsen, M. Effects of iron oxide incorporation for long term cell tracking on MSC differentiation *in vitro* and *in vivo*. *Biochem. Biophys. Res. Commun.*, **2008**, *369*, 1076-1081.

[53] Guzman, R.; Uchida, N.; Bliss, T.M.; He, D.; Christopherson, K.K.; Stellwagen, D.; Capela, A.; Greve, J.; Malenka, R.C.; Moseley, M.E.; Palmer, T.D.; Steinberg, G.K. Long-term monitoring of transplanted human neural stem cells in developmental and pathological contexts with MRI. *Proc. Natl. Acad. Sci. USA*, **2007**, *104*, 10211-10216.

[54] Wang, L.; Deng, J.; Wang, J.; Xiang, B.; Yang, T.; Gruwel, M.; Kashour, T.; Tomanek, B.; Summer, R.; Freed, D.; Jassal, D.S.; Dai, G.; Glogowski, M.; Deslauriers, R.; Arora, R.C.; Tian, G. Superparamagnetic iron oxide does not affect the viability and function of adipose-derived stem cells, and superparamagnetic iron oxide-enhanced magnetic resonance imaging identifies viable cells. *Magn. Reson. Imaging*, **2009**, *27*, 108-119.

[55] Delcroix, G.J.; Jacquart, M.; Lemaire, L.; Sindji, L.; Franconi, F.; Le Jeune, J.J.; Montero-Menei, C.N. Mesenchymal and neural stem cells labeled with HEDP-coated SPIO nanoparticles: In vitro characterization and migration potential in rat brain. *Brain. Res.*, **2008**.

[56] Sykova, E.; Jendelova, P. *In vivo* tracking of stem cells in brain and spinal cord injury. *Prog. Brain. Res.*, **2007**, *161*, 367-383.

[57] Weissleder, R.; Stark, D.D.; Engelstad, B.L.; Bacon, B.R.; Compton, C.C.; White, D.L.; Jacobs, P.; Lewis, J. Superparamagnetic iron oxide: pharmacokinetics and toxicity. *AJR. Am. J. Roentgenol.*, **1989**, *152*, 167-173.

[58] Anzai, Y.; Piccoli, C.W.; Outwater, E.K.; Stanford, W.; Bluemke, D.A.; Nurenberg, P.; Saini, S.; Maravilla, K.R.; Feldman, D.E.; Schmiedl, U.P.; Brunberg, J.A.; Francis, I.R.; Harms, S.E.; Som, P.M.; Tempany, C.M. Evaluation of neck and body metastases to nodes with ferumoxtran 10-enhanced MR imaging: phase III safety and efficacy study. *Radiology*, **2003**, *228*, 777-788.

[59] Gupta, A.K.; Curtis, A.S. Surface modified superparamagnetic nanoparticles for drug delivery: interaction studies with human fibroblasts in culture. *J. Mater. Sci. Mater. Med.*, **2004**, *15*, 493-496.

[60] Lewin, M.; Carlesso, N.; Tung, C.H.; Tang, X.W.; Cory, D.; Scadden, D.T.; Weissleder, R. Tat peptide-derivatized magnetic nanoparticles allow in vivo tracking and recovery of progenitor cells. *Nat. Biotechnol.*, **2000**, *18*, 410-414.

[61] Mailander, V.; Lorenz, M.R.; Holzapfel, V.; Musyanovych, A.; Fuchs, K.; Wiesneth, M.; Walther, P.; Landfester, K.; Schrezenmeier, H. Carboxylated superparamagnetic iron oxide particles label cells intracellularly without transfection agents. *Mol. Imaging Biol.*, **2008**, *10*, 138-146.

[62] Arbab, A.S.; Bashaw, L.A.; Miller, B.R.; Jordan, E.K.; Lewis, B.K.; Kalish, H.; Frank, J.A. Characterization of biophysical and metabolic properties of cells labeled with superparamagnetic iron oxide nanoparticles and transfection agent for cellular MR imaging. *Radiology*, **2003**, *229*, 838-846.

[63] Emerit, J.; Beaumont, C.; Trivin, F. Iron metabolism, free radicals, and oxidative injury. *Biomed. Pharmacother.*, **2001**, *55*, 333-339.

[64] Li, N.; Sioutas, C.; Cho, A.; Schmitz, D.; Misra, C.; Sempf, J.; Wang, M.; Oberley, T.; Froines, J.; Nel, A. Ultrafine particulate pollutants induce oxidative stress and mitochondrial damage. *Environ. Health Perspect.*, **2003**, *111*, 455-460.

[65] Thorek, D.L.; Tsourkas, A. Size, charge and concentration dependent uptake of iron oxide particles by non-phagocytic cells. *Biomaterials*, **2008**, *29*, 3583-3590.

[66] Arbab, A.S.; Yocum, G.T.; Wilson, L.B.; Parwana, A.; Jordan, E.K.; Kalish, H.; Frank, J.A. Comparison of transfection agents in forming complexes with ferumoxides, cell labeling efficiency, and cellular viability. *Mol. Imaging*, **2004**, *3*, 24-32.

[67] Park, I.K.; Ng, C.P.; Wang, J.; Chu, B.; Yuan, C.; Zhang, S.; Pun, S.H. Determination of nanoparticle vehicle unpackaging by MR imaging of a T(2) magnetic relaxation switch. *Biomaterials*, **2008**, *29*, 724-732.

[68] Yoo, H.S.; Park, T.G. Folate-receptor-targeted delivery of doxorubicin nano-aggregates stabilized by doxorubicin-PEG-folate conjugate. *J. Control. Release*, **2004**, *100*, 247-256.

[69] Hong, G.; Yuan, R.; Liang, B.; Shen, J.; Yang, X.; Shuai, X. Folate-functionalized polymeric micelle as hepatic carcinoma-targeted, MRI-ultrasensitive delivery system of antitumor drugs. *Biomed. Microdevices*, **2008**, *10*, 693-700.

[70] Clement, O.; Siauve, N.; Cuenod, C.A.; Frija, G. Liver imaging with ferumoxides (Feridex): fundamentals, controversies, and practical aspects. *Top. Magn. Reson. Imaging*, **1998**, *9*, 167-182.

[71] McLachlan, S.J.; Morris, M.R.; Lucas, M.A.; Fisco, R.A.; Eakins, M.N.; Fowler, D.R.; Scheetz, R.B.; Olukotun, A.Y. Phase I clinical evaluation of a new iron oxide MR contrast agent. *J. Magn. Reson. Imaging.*, **1994**, *4*, 301-307.

[72] Reimer, P.; Marx, C.; Rummeny, E.J.; Muller, M.; Lentschig, M.; Balzer, T.; Dietl, K.H.; Sulkowski, U.; Berns, T.; Shamsi, K.; Peters, P.E. SPIO-enhanced 2D-TOF MR angiography of the portal venous system: results of an intraindividual comparison. *J. Magn. Reson. Imaging*, **1997**, *7*, 945-949.

[73] Simon, G.H.; von Vopelius-Feldt, J.; Fu, Y.; Schlegel, J.; Pinotek, G.; Wendland, M.F.; Chen, M.H.; Daldrup-Link, H.E. Ultrasmall supraparamagnetic iron oxide-enhanced magnetic resonance imaging of antigen-induced arthritis: a comparative study between SHU 555 C, ferumoxtran-10, and ferumoxytol. *Invest. Radiol.*, **2006**, *41*, 45-51.

[74] Li, W.; Tutton, S.; Vu, A.T.; Pierchala, L.; Li, B.S.; Lewis, J.M.; Prasad, P.V.; Edelman, R.R. First-pass contrast-enhanced magnetic resonance angiography in humans using ferumoxytol, a novel ultrasmall superparamagnetic iron oxide (USPIO)-based blood pool agent. *J. Magn. Reson. Imaging*, **2005**, *21*, 46-52.

[75] Hahn, P.F.; Stark, D.D.; Lewis, J.M.; Saini, S.; Elizondo, G.; Weissleder, R.; Fretz, C.J.; Ferrucci, J.T. First clinical trial of a new superparamagnetic iron oxide for use as an oral gastrointestinal contrast agent in MR imaging. *Radiology*, **1990**, *175*, 695-700.

[76] Wagner, S.; Schnorr, J.; Pilgrimm, H.; Hamm, B.; Taupitz, M. Monomer-coated very small superparamagnetic iron oxide particles as contrast medium for magnetic resonance imaging: preclinical in vivo characterization. *Invest. Radiol.*, **2002**, *37*, 167-177.

[77] Turetschek, K.; Huber, S.; Helbich, T.; Floyd, E.; Tarlo, K.S.; Roberts, T.P.; Shames, D.M.; Wendland, M.F.; Brasch, R.C. Dynamic MRI enhanced with albumin-(Gd-DTPA)30 or ultrasmall superparamagnetic iron oxide particles (NC100150 injection) for the measurement of microvessel permeability in experimental breast tumors. *Acad. Radiol.*, **2002**, *9*(Suppl 1), S112-4.

[78] Delcroix, G.J.; Jacquart, M.; Lemaire, L.; Sindji, L.; Franconi, F.; Le Jeune, J.J.; Montero-Menei, C.N. Mesenchymal and neural stem cells labeled with HEDP-coated SPIO nanoparticles: in vitro characterization and migration potential in rat brain. *Brain Res.*, **2009**, *1255*, 18-31.

[79] Zhang, Z.; van den Bos, E.J.; Wielopolski, P.A.; de Jong-Popijus, M.; Bernsen, M.R.; Duncker, D.J.; Krestin, G.P. *In vitro* imaging of single living human umbilical vein endothelial cells with a clinical 3.0-T MRI scanner. *MAGMA*, **2005**, *18*, 175-185.

[80] Pisanic, T.R., 2nd; Blackwell, J.D.; Shubayev, V.I.; Finones, R.R.; Jin, S. Nanotoxicity of iron oxide nanoparticle internalization in growing neurons. *Biomaterials.*, **2007**, *28*, 2572-2581.

[81] Hsiao, J.K.; Chu, H.H.; Wang, Y.H.; Lai, C.W.; Chou, P.T.; Hsieh, S.T.; Wang, J.L.; Liu, H.M. Macrophage physiological function after superparamagnetic iron oxide labeling. *NMR. Biomed.*, **2008**, *21*, 820-829.

[82] Hussain, S.M.; Hess, K.L.; Gearhart, J.M.; Geiss, K.T.; Schlager, J.J. *In vitro* toxicity of nanoparticles in BRL 3A rat liver cells. *Toxicol. In Vitro*, **2005**, *19*, 975-983.

[83] Schafer, R.; Kehlbach, R.; Wiskirchen, J.; Bantleon, R.; Pintaske, J.; Brehm, B.R.; Gerber, A.; Wolburg, H.; Claussen, C.D.; Northoff, H. Transferrin receptor upregulation: in vitro labeling of rat mesenchymal stem cells with superparamagnetic iron oxide. *Radiology*, **2007**, *244*, 514-523.

[84] Huang, D.M.; Hsiao, J.K.; Chen, Y.C.; Chien, L.Y.; Yao, M.; Chen, Y.K.; Ko, B.S.; Hsu, S.C.; Tai, L.A.; Cheng, H.Y.; Wang, S.W.; Yang, C.S.; Chen, Y.C. The promotion of human mesenchymal stem cell proliferation by superparamagnetic iron oxide nanoparticles. *Biomaterials*, **2009**, *30*, 3645-3651.

[85] Mahmoudi, M.; Simchi, A.; Milani, A.S.; Stroeve, P. Cell toxicity of superparamagnetic iron oxide nanoparticles. *J Colloid Interface Sci.*, **2009**, *336*, 510-518.

[86] Karlsson, H.L.; Gustafsson, J.; Cronholm, P.; Möller, L. Size-dependent toxicity of metal oxide particles—A comparison between nano- and micrometer size. *Toxicol. Lett.*, **2009**, *188*, 112-118.

[87] Schäfer, R.; Kehlbach, R.; Müller, M.; Bantleon, R.; Kluba, T.; Ayturan, M.; Siegel, G.; Wolburg, H.; Northoff, H.; Dietz, K.; Claussen, C.D.; Wiskirchen, J. Labeling of human mesenchymal stromal cells with superparamagnetic iron oxide leads to a decrease in migration capacity and colony formation ability. *Cytotherapy*, **2009**, *11*, 68-78.

Received: October 19, 2009 Revised: December 12, 2009 Accepted: December 18, 2009